POLITECNICO DI TORINO
Repository ISTITUZIONALE

Analysis of borehole guided waves for geotechnical application

Availability:
This version is available at: 11583/2858302 since: 2020-12-18T11:39:11Z

Published
DOI:

(Article begins on next page)

16 July 2022

Analysis of borehole guided waves for geotechnical application

A. Godio[1] and C. Strobbia[2]

[1] DITAG, Politecnico di Torino, Italy
[2] EUCENTRE, Pavia, Italy

ABSTRACT   The reliability of Stoneley waves (SWs) is discussed for the characterisation of the mechanical properties of soft and hard rock in borehole seismic techniques using source on the surface and hydrophones as receivers. The SWs propagate along the fluid-filled borehole; the propagation is affected by the mechanical and hydraulic properties of the fluid and the surrounding medium. At low frequencies, in a non-diffusive medium (impermeable formation), the wave velocity depends on the density, the wave velocity of the fluid and the shear modulus of the formation. The models adopted to infer the wave velocity in elastic formations in uncased and cased boreholes are discussed. We discuss two examples to check the discrepancies between the theoretical and the experimental evidence. The presence of casing in soft rock greatly reduces the sensitivity of the SW propagation to the mechanical properties of the medium. In hard rock, the scattering of the primary wavefields could be adopted to detect the presence of rock mass discontinuities (fractures).

1. Introduction

Seismic wave propagation in a fluid-filled borehole was studied in detail by Biot (1952). The ratio of shear wave velocity in the solid and compressional velocity in the fluid, the density contrast between fluid and solid, and the seismic wavelength-to-borehole diameter ratio are all critical parameters for seismic wave propagation. The coexistence of the interface wave, the Stoneley wave (SW), and the dispersive (reflected) modes for a wide range of seismic wavelengths is well known (Paillet and White, 1982). In geophysical exploration for petroleum, the SWs are usually considered as coherent noise, because they can mask the correct observation of direct and reflected events. On the other hand, in geotechnical applications the propagation of SWs can be analysed to estimate the mechanical parameters of the formation and detect the presence of geological interfaces.

Theoretical relationships between SW propagation in boreholes and geotechnical parameters, such as shear elastic modulus or permeability, are well established in hydrocarbon prospecting. Moreover, Tang (2002) studied the formation of shear-wave transverse isotropy from borehole SW measurements.

The velocity of surface waves in boreholes is related to the mechanical parameters of the rock skeleton and fluid-matrix interaction effects; in dry conditions, the velocity is linked to the density and shear velocity of the medium. In a wet porous medium, the fluid-matrix interaction leads to a complex non-elastic behaviour; in such a case, the velocity also depends on the diffusivity term.

Attenuation data are not routinely used to determine rock properties because it is very difficult to obtain accurate attenuation measurements, from either seismic or well-logs. Attenuation is

potentially more sensitive than velocity to the amount of gas in a rock. Both velocity and attenuation have been used to estimate formation permeability from borehole SWs (Cheng *et al*., 1987). High permeability decreases velocity and increases attenuation, as proved by theoretical models and laboratory experiments (Winkler and Murphy, 1995, Norris, 1989).

In near surface geotechnical applications, the requirement of an alternative and accurate way of estimating shear properties and rock permeability, taking into account the casing effects, the damage to the hole due to drilling and, the presence of drainage material in the annulus, is a challenge; moreover, in downhole or vertical seismic profile (VSP) investigations, the presence of high-amplitude signals associated to guide waves could mask the reconnaissance of direct compressional and shear waves and reflected wavefields. Techniques to model and extract the guided wave are, therefore, necessary to separate the different wavefields in a full waveform analysis of downhole data. The classical separation of the different wavefields has been adopted in the present work using the tau-pi transform (Hu and McMechan, 1987).

In this paper, we explore the effectiveness of using guided waves in boreholes for geotechnical purpose; an attempt is also made to analyse the reliability for near surface applications in both loose sediments and in hard rock. The paper considers also the main theoretical aspects that refer to velocity and attenuation in cased and uncased boreholes.

The reliability of the propagation of SWs in vertical and horizontal boreholes for geotechnical characterization at shallow depth is discussed. Some theoretical aspects of the propagation are introduced. The theoretical analysis is synthetically described considering the different behaviour of SWs in soft rock and hard rock; soft rock indicates a medium characterized by a shear wave velocity lower than the fluid velocity; hard rocks are characterised by shear waves velocity values higher than the fluid velocity. Wave velocity dispersion with frequency is considered taking into account the mechanical properties of the surrounded medium, the fluid characteristics and the borehole diameter. The results of the theoretical simulation are discussed and compared with the results of two selected examples; the first one refers to downhole data acquisition in a cased borehole in a porous medium (soft rock); the second refers to the acquisition in a horizontal borehole (without casing) that permitted the diffraction effects of SWs to be analysed to detect the main rock mass discontinuities in hard rock.

2. Theorethical background

2.1. Body waves in borehole techniques

In most shallow borehole seismic techniques for geotechnical applications, the sources are located on the surface while receivers are placed in the borehole (downhole test): this scheme is also widely adopted in deep exploration to calibrate the seismic section. According to this layout, the wavefield generated by the source, composed of body P- and S-waves, is propagated down into the Earth and is refracted and reflected by the existing interfaces and impedance variations. The energy propagating from the source downwards to the receivers is referred to as the down going wavefield. The up going wavefield is composed of the events reflected by the interfaces at different depths, within the borehole range and below it. In a single shot point gather (Fig. 1), the upgoing wavefield can be easily recognised because the first arrivals of the wave are aligned on the reverse direction of the downgoing wavefield; therefore, the separation between the two wavefields is easier than in
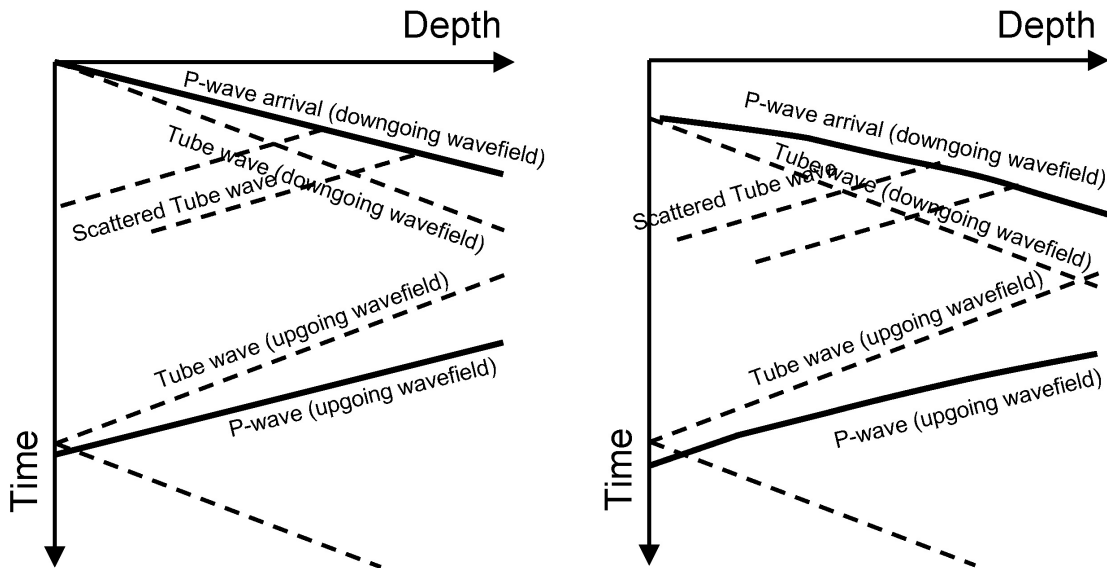
Fig. 1 - First arrivals of different wavefields from a shot on the surface at zero offset (left) and non-zero offset (right); the scattering of tube waves is caused by the change in the impedance along the borehole due to hole discontinuities of rock mass and hole irregularities.

surface reflection profiling. Body waves propagating in the formation can be detected since they are transmitted across the interface of the borehole (coupling coefficient).

2.2. Stoneley waves

The presence of a free surface at a boundary or within a solid or liquid medium, makes the existence of surface waves propagating along the surface. Two main mechanisms generate the SWs at the top of the water column inside the borehole: the conversion of body waves (mainly compressional waves) in the surface wave at the air-water interface and the conversion of the surface wave in the SW at the same interface. These mechanisms provide different SW wave-fields, called primary and secondary.

The particle displacement of surface waves is perpendicular to their direction of propagation (transverse waves) and the amplitude of displacement falls off rapidly in directions that are normal to (at a right angle to) the surface along which it is propagating. The energy of a surface wave is confined to a region of one or two wavelength depths from the surface.

The cylindrical surface of a borehole in a solid medium makes it possible for a different kind of surface wave to exist: SWs are surface waves that propagate along a fluid filled borehole, in the direction coincident to the borehole axis, and a particle motion in the filling fluid which is normal to both the surface (radial) and the long axis of the borehole.

The SW propagation is affected by the elastic and hydraulic properties of the fluid and the surrounding formation: the casing, apart from influencing the elastic properties of the system to a great extent, can be an impermeable barrier between the borehole and the formation.

The theory of wave propagation in boreholes filled with fluid is well known; Biot (1952)

described unattenuated waves that propagate along a stress-free borehole and obtained a relationship between the frequency and the phase velocity. In general, the set of interfacial waves is composed of Pseudo Rayleigh (reflected) waves and SWs (Cheng and Toksoz, 1981); the first is highly dispersive, while the second shows very little dispersion. Moreover, Pseudo Rayleigh waves have very high cut-off frequencies, and are not present with the high wavelength λ of downhole data in the low frequency band (less than 1 kHz).

The main wavefield of a SW is generated on the upper surface of a fluid column by the conversion of compressional or Rayleigh waves; secondary wavefields can be observed, starting from the bottom of the borehole, or in the presence of discontinuities along the boreholes (changes in the diameter, changes in the mechanical properties, the presence of fractures). Strong impedance contrasts across the borehole can generate SWs that interact with body waves, and can also cause scattering phenomena. SWs are reflected when the cross sectional area undergoes impedance changes, and all the energy is reflected at the bottom. Scattering of tube waves can be used to show the presence of fractures, washout zones or diameter changes (Kostek *et al.*, 1998).

SW amplitudes decrease exponentially in the radial direction and there is a very limited attenuation in the axial direction; their energy remains at a high level over long distances, mainly due to the absence of the geometrical spreading factor. The attenuation factor for these guided waves depends mainly on the shear wave attenuation factor of the formation and on the attenuation of the wave in the fluid.

2.2.1. Low frequency SWs in impermeable media

The frequency content of propagating signals in a seismic survey makes the dominant wavelength much longer than the borehole dimension: in these conditions, the phase velocity of SWs becomes independent from the frequency for large values of λ/D, where D is the borehole radius, the phenomenon is quasi static and coincides with the water hammer. According to these hypotheses, the relation between the elastic properties and velocity c in a fluid for cased and uncased boreholes is (White, 1983):

$$c = \frac{\sqrt{K/\rho}}{\sqrt{1 + \dfrac{2K}{R}\dfrac{dR}{dp}}} \tag{1}$$

where K and ρ are the bulk modulus and fluid density, R is the borehole radius and p is the inner pressure.

The term dR/dp includes the mechanical properties of the medium, as the radial deformation is due to pressure variations. It is essentially related to the shear modulus of the formation around the borehole, and when radial heterogeneities are present, it depends on the properties of the different concentric layers, as it is more sensitive to inner rings. Since R, K and ρ are often known, the SW velocity can be used directly to estimate the average elastic properties of the formation.

The cross-sectional area around the borehole that influences the tube wave propagation is limited to only a few borehole radii; concentric discontinuities, such as a weak cementing zone around the casing or fracturing close to the hole, act as a boundary of the zone of influence (see Appendix A).

2.2.1.1. Uncased borehole

The SW velocity in uncased boreholes can be used to estimate the mechanical properties of the formation directly. In more general conditions, the SW velocity in slow formations is affected much more by the shear modulus than by other fluid or medium parameters (Stevens and Day, 1986). Moreover, the SW velocity can indicate the mechanical damage and radial anisotropy induced by stress relief (Renlie and Raaen, 1993). The zone close to a borehole drilled in a hard rock presents poor mechanical properties, and the amount of damage can be evaluated by comparing the modulus inferred from the down going shear wave velocity with the modulus inferred from the SW velocity.

2.2.1.2. Cased boreholes

In cased boreholes, the SWs are sensitive to the elastic properties of the medium only if a good coupling between the casing and the geological formation is guaranteed; otherwise (weak coupling) the SW velocity depends on the mechanical properties of the casing system. A stiff casing greatly reduces the radial deformation, and the stiffness of the formation can be mobilised only if a good coupling with the casing is assured.

2.2.2. High frequency Stoneley waves

The signals that have to be considered for well logging have much higher frequencies, and the low frequency approximation does not apply: moreover, SWs are dispersive, like most surface waves. The effect of hard rock on the SW velocity can be negligible due to the low compressibility of the rock mass. In such a case, the velocity is mainly affected by the fluid velocity and approximates the compressional velocity of the fluid itself.

The dispersive character of SWs could be useful to estimate shear velocity (Mari *et al.*, 1996; Burns *et al.*, 1992) and to determine rock mass permeability (Norris, 1989). The approach suggested by Mari *et al.* (1996) considers the relation between the phase velocity at different frequencies and the zero-frequency SW velocity. Tezuka *et al.* (1997) consider the effect of the borehole and tool diameter to compute the SW velocity at different frequencies:

$$
\frac{I_0(fr)}{I_1(fr)} + \frac{I_1(fr_t)}{I_1(fr)}\frac{K_0(fr)}{K_1(fr_t)} + \left\{1 - \frac{I_1(fr_t)}{I_1(fr)}\frac{K_0(fr)}{K_1(fr_t)}\right\} \times
$$

$$
\frac{\rho}{\rho_f}\frac{f}{n}\left[\left(\frac{2v_s^2}{c^2}-1\right)^2\frac{K_0(nr)}{K_1(nr_t)} - \frac{2v_s^2 n_m}{c^2 k^2}\left(\frac{1}{mr}+\frac{2v_s^2}{c^2}\frac{K_0(mr)}{K_1(mr)}\right)\right] = 0
$$

$$
n = \sqrt{k^2 - \omega^2/v_p^2}
$$

$$
m = \sqrt{k^2 - \omega^2/v_s^2}
$$

$$
f = \sqrt{k^2 - \omega^2/v_f^2}
$$

(2)

where $m, n,$ and f are the radial wavenumber, $I_0, I_1, K_0,$ and K_1 are the modified Bessel function of order 0 and 1, k is the wavenumber of the SW, r is the borehole radius; r_t is the radius of the logging tool, ρ is the rock mass density, ρ_f is the fluid density, Vs and Vp are the S-wave and P-wave velocities, $c = \omega/k$ is the phase velocity of the SW and $\omega = 2\pi f$ is the angular frequency of the

acoustic impulse. This recursive formula permits, once the P-wave and SW velocities have been estimated, the S-wave velocity to be computed, considering both the effect of the borehole size and the disturbance due to the presence of the geophones or hydrophones.

2.2.3. Attenuation and dispersion

The attenuation of the SW in the presence of pore-fluid mobility is well known and it has been proposed as a means of measuring permeability (Alhilali and Zemanek, 1984). Quantitative modeling by Rosenbaum (1974), Schmitt and Bouchon (1984), and by Schmitt *et al*. (1988) supports the conclusion that attenuation increases with permeability and with pore fluid mobility; i.e., attenuation decreases as pore-fluid viscosity increases.

In the quasi-static regime, tube-wave dissipation results from the diffusion of pore pressure in the surrounding formation via the connected pore network (White, 1983). This dissipative mechanism is still effective at higher frequencies, as confirmed by Rosenbaum (1974); the mechanism is complicated by the coupling between pore pressure diffusion and the purely geometrical dispersive effects found in elastic formations.

The tube wave, or low-frequency manifestation of the SW, was modelled using the quasi-static approximation (e.g. Mathieu, 1984); Norris (1989) included the effect of the formation matrix compressibility, which tends to marginally increase the tube-wave attenuation; a fully dynamic description was furnished using the Biot theory of poroelasticity.

The dispersion derived from Biot's equations reduces to the quasi-static dispersion relation in the low-frequency limit. Comparisons of the quasi-static and dynamic theories for water infiltration in typical sandstones show that the former are a good approximation for at least 1 kHz. The Biot theory, where attenuation and dispersion are maximum, is often of the order of 100 kHz. Increasing viscosity pushes the critical frequency even higher. Seismic waves and sonic logging are, therefore, almost always in the low-frequency range of the Biot theory.

For typical sandstones, the Biot theory predicts a maximum of one to two percent velocity dispersion between its low and high-frequency limits (Winkler, 1985). The predicted attenuation is also rather small, with a minimum of quality factor (Q) of the order of 100.

An interesting prediction of the Biot theory is the existence of a second compressional wave dominated by the properties of the pore fluid (often called the Biot slow wave). This wave is diffusive at low frequencies and it is propagatory at high frequencies.

3. Parametric analysis

The relationship (2) permits the SW behaviour to be explored, starting from the geotechnical data of the medium around the borehole, expressed in terms of P-wave and S-wave velocities and bulk density; the recursive formula is used to compute the SW velocity, considering both the effect of the borehole size and the disturbance due to the presence of the logging tool. We have performed the simulation for the different model parameters as indicated in Table 1. The models 1-3 refer to hard rock with P-wave velocity in the 5000-6000 m/s range and shear wave velocity varying between 3000 and 3600 m/s. Models 4-6 simulate a low consolidated soft rock with high ratio between the P-wave velocity and S-wave velocity; the density values range from 1300 to 1800 kg/m^3.

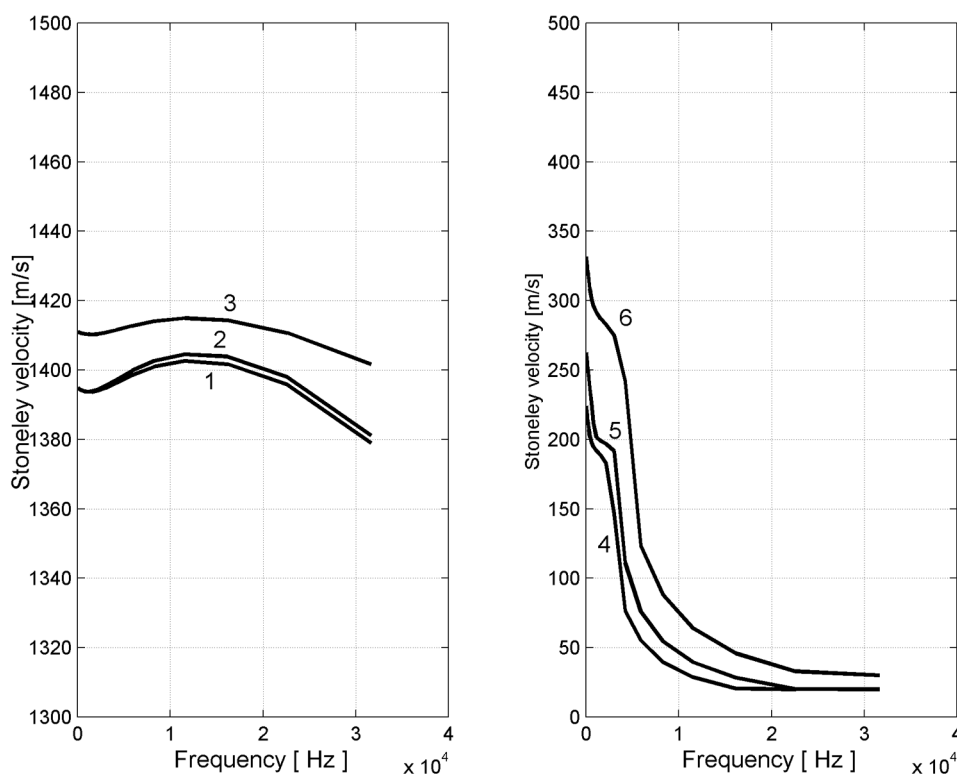The simulation involves the computation of the phase velocity with respect to the frequency for

Fig. 2 - Dispersion of the phase velocity of the SW for different values of mechanical properties of the formation; see Table 1 for the model parameters of density and P – and S-wave velocity values: a) in hard rock; b) soft rock.

a fixed borehole radius (0.05 m) and tool size (radius = 0.02 m) configuration in a borehole without casing.

The plots in Figs. 2a and 2b show the phase velocity curves versus frequency for soft and hard rock adopting different mechanical properties of geological formations. It can be noted that, in slow formations, according to relationship (2) and considering the elastic behaviour, the SW velocity is mainly sensitive to the shear wave velocity and secondary to the density.

At low frequency (below 1 kHz), in the range of the standard downhole investigation for geotechnics, the phase velocity shows a slight dispersion with frequency. An abrupt decrease in velocity is reported at a cut-off frequency of about 3 kHz. A strong dispersive behaviour is depicted in the 3 kHz to 20 kHz frequency range, which is the standard frequency range adopted in the commercial logging tools.

In hard rock, the sensitivity to the bulk density and to the compressional wave velocity of the formation is negligible; as far as the sensitivity to the shear wave velocity is concerned, an increase of 20% in the shear velocity determines a change in the SW velocity of less than 5% in a wide frequency range.

An evaluation of the effect of the annulus material between the PVC casing and the borehole can be assessed by computing the theoretical velocity value (see Appendix A).

Table 1 - Rock mass and fluid parameters adopted for the SW velocity analysis, with respect to the frequency.

		Vp	Vs	Fluid velocity [m/s]	Rock density [kg/m3]	Fluid density [kg/m3]	Borehole radius [m]	Tool radius [m]
Hard rock	**Model 1**	5000	3000	1450	2900	1000	0.05	0.02
	Model 2	6000	3600	1450	2900	1000	0.05	0.02
	Model 3	5000	3600	1450	2900	1000	0.05	0.02
Soft rock	**Model 4**	2000	200	1450	1800	1000	0.05	0.02
	Model 5	2000	200	1450	1300	1000	0.05	0.02
	Model 6	2000	300	1450	1300	1000	0.05	0.02

Starting from the geometrical characteristics of the borehole (inner casing radius = 0.055 m, external casing radius = 0.065 m, borehole radius = 0.08 m) the model sensitivity to the elastic parameter of PVC casing, to the annulus mechanical properties and the embedded medium can be estimated. The simulation of the model sensitivity to the PVC casing is given in Fig. 3, where the mechanical properties of PVC are E= 2-3 GPa, Poisson coefficient = 0.38) and the Young modulus of the formation is Eformation=2 GPa. The response of the SW velocity in the selected range of the elasticity modulus varies between 740 m/s and 780 m/s; an increase of 50% in the value of the casing modulus provides for an increase of 5% in the wave velocity.

As far as the model sensitivity to the annulus material in the aforementioned borehole geometrical configuration is concerned, we computed the response for a model of three concentric layers (thin casing, annulus and homogeneous medium with radial infinite extension). A low value of the Young's modulus of the material filling the annulus has been considered (Ea=0.1 GPa – 2 GPa) and a Poisson coefficient of 0.3. The casing parameter are: Ecasing= 2 GPa – Poisson coefficient = 0.38; for the formation we adopted Eformation = 0.1 GPa and Poisson coefficient 0.45. The results are plotted in Fig. 4; the SW velocity ranges from 430 m/s to 650 m/s.

The dispersion with frequency appears negligible in the frequency range commonly adopted in seismic and acoustic investigation. The SW velocity appraises the fluid velocity (1450 m/s). It is clear that the approach to estimate shear wave velocity starting from experimental data of SWs would be greatly affected by experimental uncertainties to a great extent.

4. Analysis of downhole data: experimental results

This paragraph refers to downhole low frequency experiments in soft and hard rock in cased borehole and uncased borehole.

The first test refers to the downhole seismic measurement using both hydrophones and triaxial geophones in porous sediments. The geological set up of the area consists of a Quaternary deposit from a lacustrial depositional environment. The geological sequence of the first 50 m in depth shows a near surface formation of lake peat, shale and sandy deposits. Core samples and
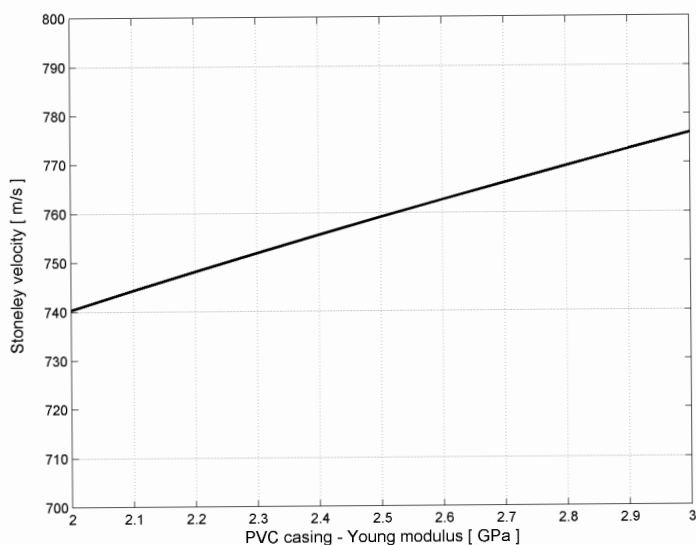
Fig. 3 - Synthetic response of the SW velocity versus Young's modulus of the PVC casing with inner radius of 0.055 m, external radius of 0.065 m and Eformation=2 GPa.

mineralogical analysis performed on different specimens pointed out that quartz is prevalent in a percentage of more than 80% in the lake peat, in the shale and in the sandy material.

Seismic measurements were conducted in a 40 meter borehole deep according to two different schemes: downhole, with a single shot close to the borehole head using a string of four triaxial geophones and a walkaway VSP using a string of hydrophones (Fig. 5). The borehole consists of a drilling of 127 mm and a PVC casing of 3 inches. The porosity of the sediments was inferred from laboratory analysis performed on core samples; an average value of 0.65 was detected for the shaly formations; the lake peat was characterised by an average porosity value of 0.4.

Accurate wave-field separation in order to preserve the signal integrity is necessary to properly determine the attenuation/dispersive character of the SWs and to separate the tube wave from the records. Hu and McMechan (1987) analysed multidimensional wave-field transformations to wave-field re-sampling, interpolation and extrapolation, separation of P- and S-waves, separation of up-going and down-going waves and tube wave removal techniques in VSP. The inherent symmetry of the tau-pi image offers a useful tool to separate the down-going and up-going wave-fields. Tube wave energy and body wave energy are distributed symmetrically in the slowness dimension. The recommended method for separating tube waves is to isolate and remove the body wave in the tau-pi domain and then to transform it back into the time-depth domain; when a large number of reflections is present, the method is impractical and other approaches are suggested (Hu and Mechan, 1987). In the present approach, the tau-pi analysis permitted the different down-going and up-going SW to be well-separated, because of the higher energy compared to the body waves.

The analysis of SW velocity through a regression analysis performed on the time-depth diagram shows that the best fitting is obtained for a velocity value of 418 +/- 3 m/s; to improve the robustness of the statistical evaluation the regression analysis was performed both on the direct wave-fields and the waves reflected from the borehole bottom.
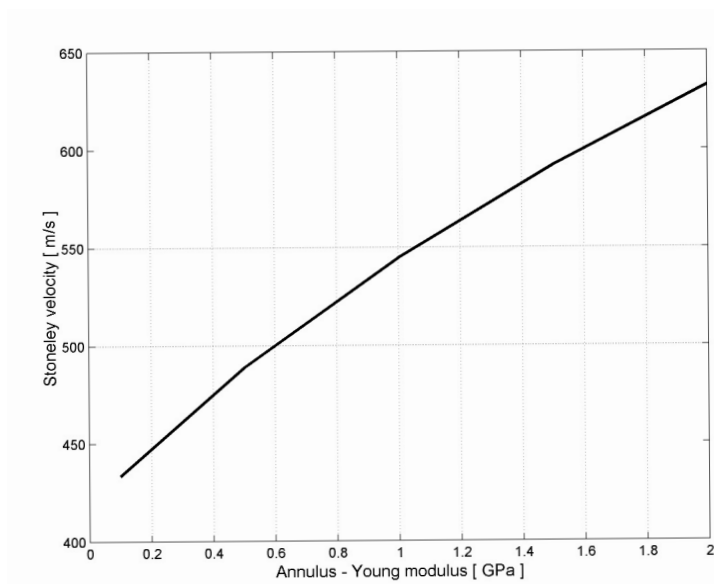
Fig. 4 - Sensitivity of the SW velocity versus the elasticity modulus of the annulus for a borehole with a PVC casing with the inner radius of 0.055 m, external radius of 0.065 m and Epvc=2 GPa and Eformation=0.1 GPa.

An attempt to model the effective SW velocity, recorded in the cased borehole, was made. We found a good sensitivity to the formation parameters only if the annulus is filled with unconsolidated material, as pointed out by the sensitivity analysis performed in the previous paragraph (Eannulus < 0.1 GPa); this hypothesis appears to be realistic in the test site, as the presence of the groundwater level at 3 meters below the surface might cause a low consolidation of the concrete along the annulus. The computation of the theoretical value of the SW using the parameters indicated in Table 2 provides a wave velocity of about 420 m/s.

The attenuation analysis was carried out after picking the amplitude of the in-phase peaks of the Stoneley wavelet; the regression analysis was performed in a linear-log domain to make the relationship between the amplitude and the depth linear (Fig. 6). The main frequency of the Stoneley wavelet was estimated by analysing the semi-period of the Stoneley wavelet in the time domain. A more accurate frequency domain analysis was neglected considering that dispersion effects are not appreciable in these records.

The quality factor (Q) of the SW is related to the attenuation coefficient by the relationship:

$$\alpha(\omega) = \frac{\pi f}{Qc} \tag{3}$$

where c is the SW velocity (about 420 m/s) and the main frequency (f) has been assumed to be about 90 Hz. The regression results show a high correlation coefficient (R^2=0.9807) for a quality factor estimated equal to 10.6 +/-0.6. The physical meanings of the attenuation factor for SWs is related to the dissipative phenomena in rock formation: a quantitative interpretation should consider the existence of dissipative phenomena due to matrix-fluid interaction and fluid mobility around the wall of the borehole.
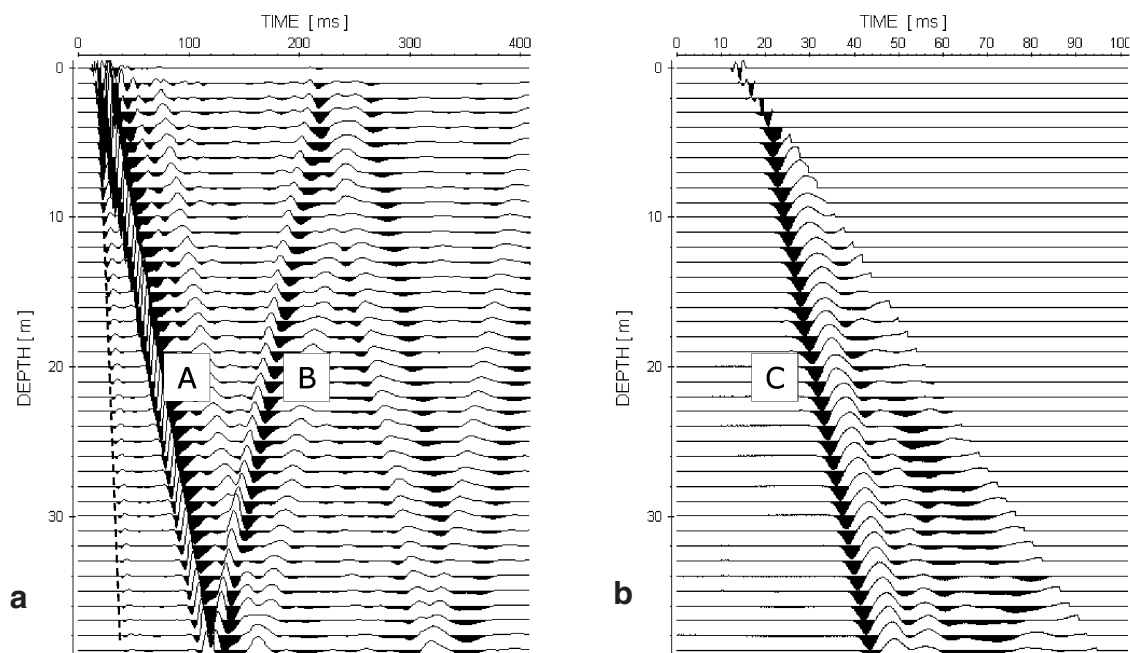
Fig. 5 - Separation of P-wave arrivals for data acquired in soft rock (test site 1) with a string of hydrophones in a water-filled borehole and the source on the surface: a) (A) - P-wave first arrival, (B) downgoing SWs; b) muting procedure allows the P-wavefield (downgoing) (C) to be separated from the SWs.

The second test concerns a borehole data acquisition, using hydrophones, in an almost horizontal borehole. The acquisition was performed in a 40 meter long uncased borehole using a string of 1 m-spaced hydrophones. The source was located at different distances from the borehole on the external wall of the rock mass. The body waves and SWs were recorded as plotted in the seismograms of Fig. 7.

The geophysical investigation was part of the geological and geotechnical characterisation of a rock mass in a landslide in an Alpine valley in northern Italy, where an estimation of the rock mass mechanical properties and detection of the fractures were required (Godio *et al*., 2006). The borehole investigation in the schist formation pointed out the presence of a rock mass characterised by velocity values of P-waves, in the 3500-4000 m/s range. The information that could be derived from the analysis of the SWs in the uncased borehole in hard rock is discussed in this context. The main wavefield of the SW is generated at the upper surface of the fluid column by the conversion of direct surface and body waves, while secondary wave-fields can be observed starting from the bottom of the borehole or in the presence of discontinuities along the boreholes. It can be noted that the SWs are characterised by an average velocity value of 1350 m/s, from the head of the hole to the coordinate 20 m; as previously mentioned in open holes and under the hypothesis that the effect of rock mass permeability is negligible, the SW velocity mainly depends on the shear modulus of the surrounding rock, and on the fluid elastic properties. Therefore, the decrease of the SW velocity from the middle to the bottom of the borehole should be related to the weakness of the mechanical properties of the rock annulus around the borehole;

Table 2 - Mechanical parameters of the casing, annulus and formation to model the theoretical SW velocity of 420 m/s according to the model in Appendix A.

	Casing	Annulus	Formation
Young's modulus	2000 MPa	50 MPa	100 MPa
Poisson coefficient	0.38	0.30	0.45

this could be caused by the borehole drilling.

The model in Appendix A was adopted to estimate the sensitivity of the SW velocity to the mechanical properties (Young's modulus) under the assumption of the presence of a perturbed annulus around the borehole due to drilling. The model response has been estimated for two different values of Young's modulus of the undisturbed rock mass (30 GPa and 40 GPa). The results are plotted in Fig. 8; it can be noted that low velocity values of SWs, as recorded in the real data between the coordinate 0 and 20 meters, is compatible with low values of the Young's modulus of the fractured annulus (Efractured < 2 GPa for a fractured radius of 0.15 m). The model response appears to be quite insensitive to the mechanical properties of the sound rock. The response is sensitive instead to the radius of the disturbed zone: the velocity value ranges from 800 m/s for an annulus radius of 0.3 m to 1100 m/s for a radius of 0.1 m.

The seismogram (Fig. 9) pointed out some diffraction events located at coordinates of 4 m, 22 m and 34 m from the borehole bottom; these events are correlated with the presence of open discontinuities, as confirmed by the analysis of the specimens, collected during the drilling. From a theoretical point of view, it is possible to relate the main features of the diffraction events to the fracture characteristics, according to Kostek *et al*. (1998). For an elastic medium with
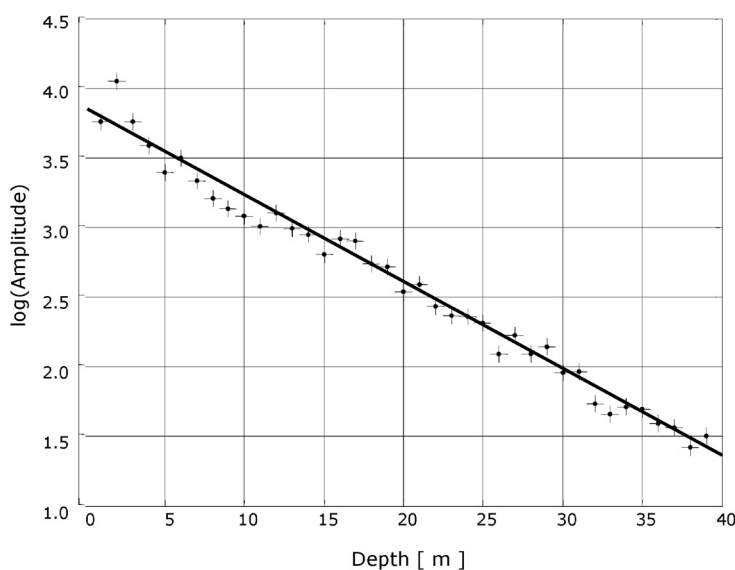

Fig. 6 - Regression analysis of the amplitude of SWs in test site 1 and estimate of the quality factor; Q=10.6 +/- 0.5 (with 95% confidence bounds of regression) – R^2=0.9807 and rmse (root mean squared error)= 0.0969, frequency = 88 Hz.
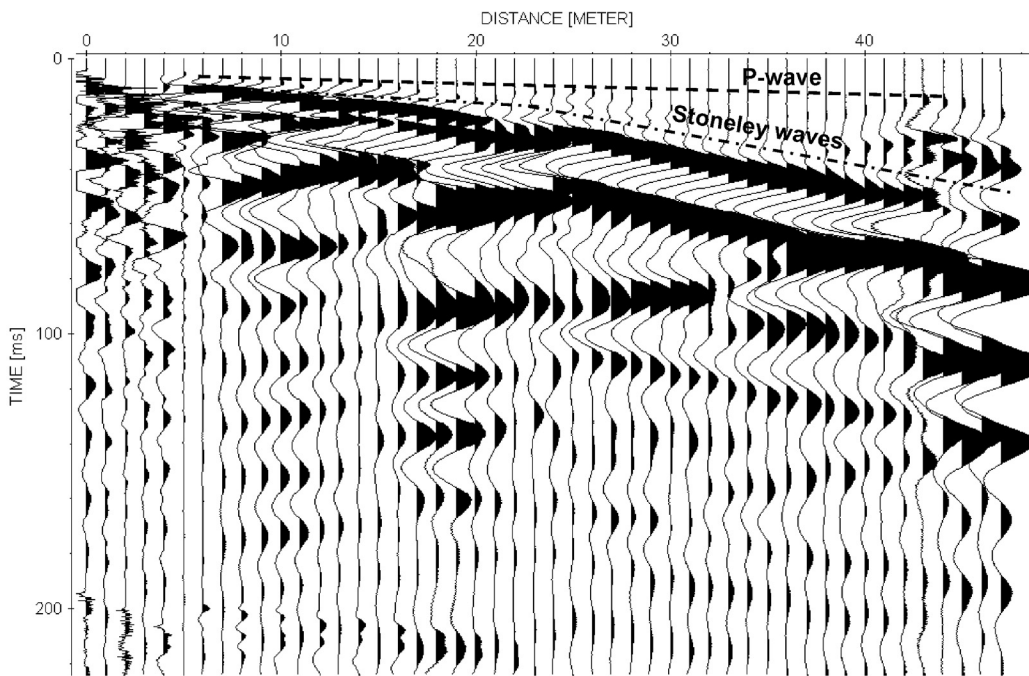
Fig. 7 - Recorded data in a horizontal borehole (second test site) and picking of the P-wave and SWs.
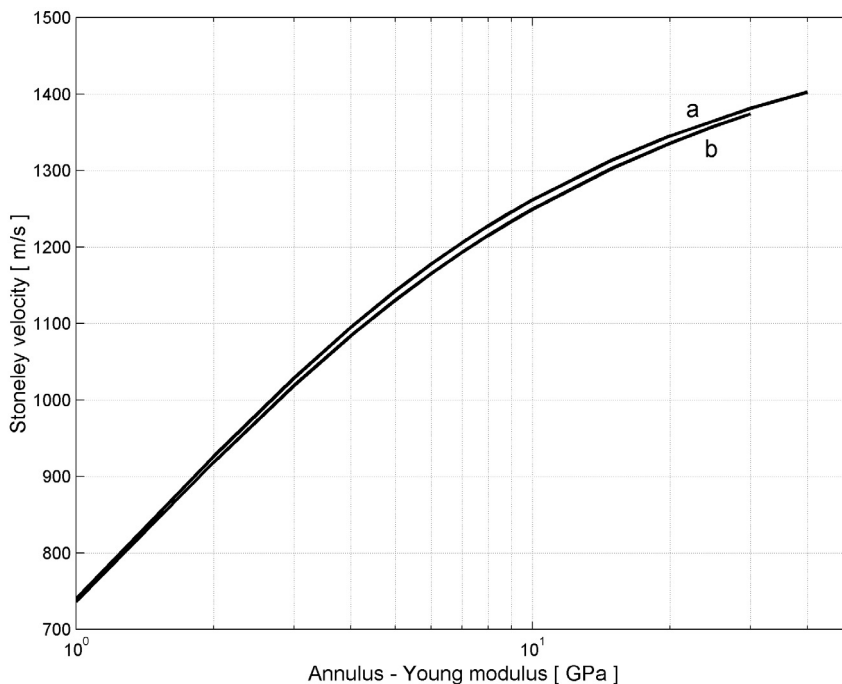

Fig. 8 - Sensitivity of the SW velocity versus the annulus (fractured zone) modulus of elasticity in hard rock for a borehole radius of 0.07 m, annulus radius of 0.15 m (Poisson coefficient = 0.3) embedded in a sound rock; a) (Eformation =30 GPa; b) Eformation =30 GPa (Poisson coefficient = 0.2).
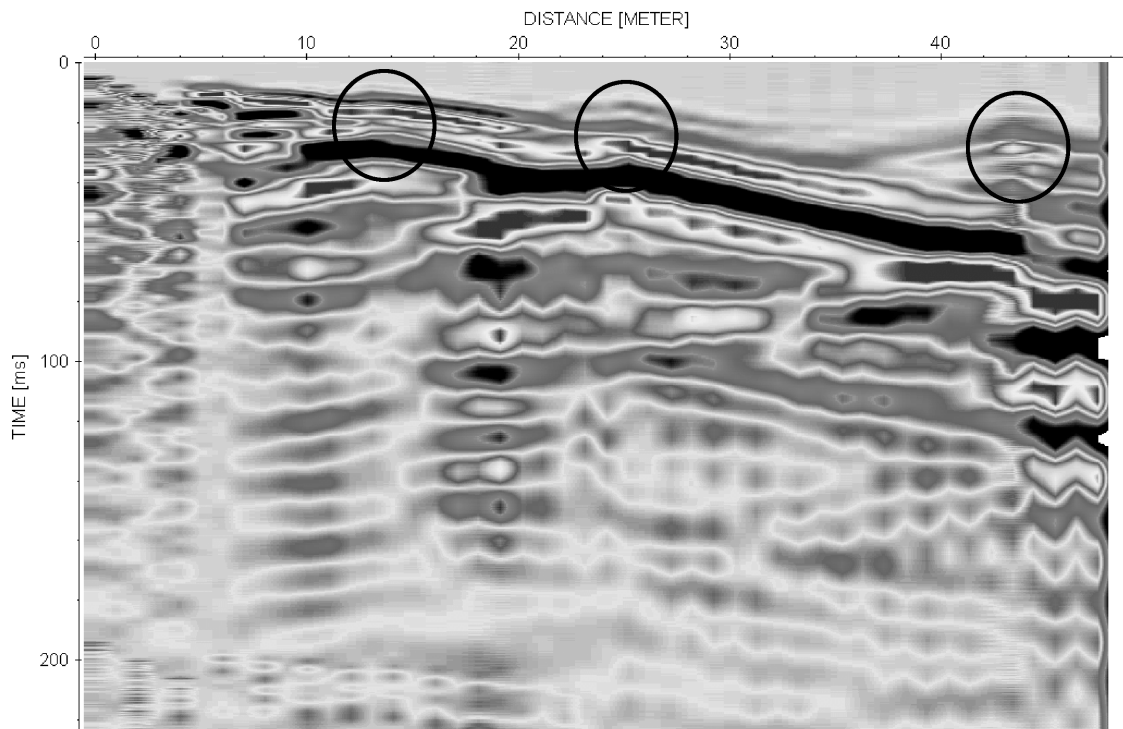
Fig. 9 - Amplitude image of the seismograms of Fig. 9 with evidence of scattering of the SWs caused by fractures along the borehole.

discontinuities perpendicular to the borehole and with a washout zone around the borehole, the amplitude of the reflection coefficient of the SW can be estimated using an analytical approach:

$$R(\omega) = \frac{i\left[kV/2\pi \cdot r^2 - dhH_1^{(1)}(kd)/r^2 H_0^{(1)}(kd)\right]}{1 - i\left[kV/2\pi \cdot r^2 - dhH_1^{(1)}(kd)/r^2 H_0^{(1)}(kd)\right]} \tag{4}$$

where H_0, H_1 are the Hankel function of order 0 and 1, k is the wavenumber of the tube waves, V is the volume of the washout zone; r is the radius of the borehole, h is the fracture aperture and d is the radial dimension of the washout zone. The wavenumber k in the fluid-filled borehole and the tube wave velocity, in the elastic formation are determined from the borehole period equation, according to relationship (2). The response of the reflection coefficient is computed by means of Eq. (4) and is plotted in Fig. 10. For low frequencies (below 200 Hz) the changes in the R coefficient amplitude is more or less 10-15% for apertures ranging from 1 cm up to 15 cm. Therefore, an accurate modelling of the aperture behaviour, starting from time domain, low frequency, experimental data, is not effective; in the range between 100 Hz to 500 Hz the spectral response of the R coefficient is very sensitive to the aperture of the discontinuities, suggesting the need of the data acquisition in a broadband frequency domain.
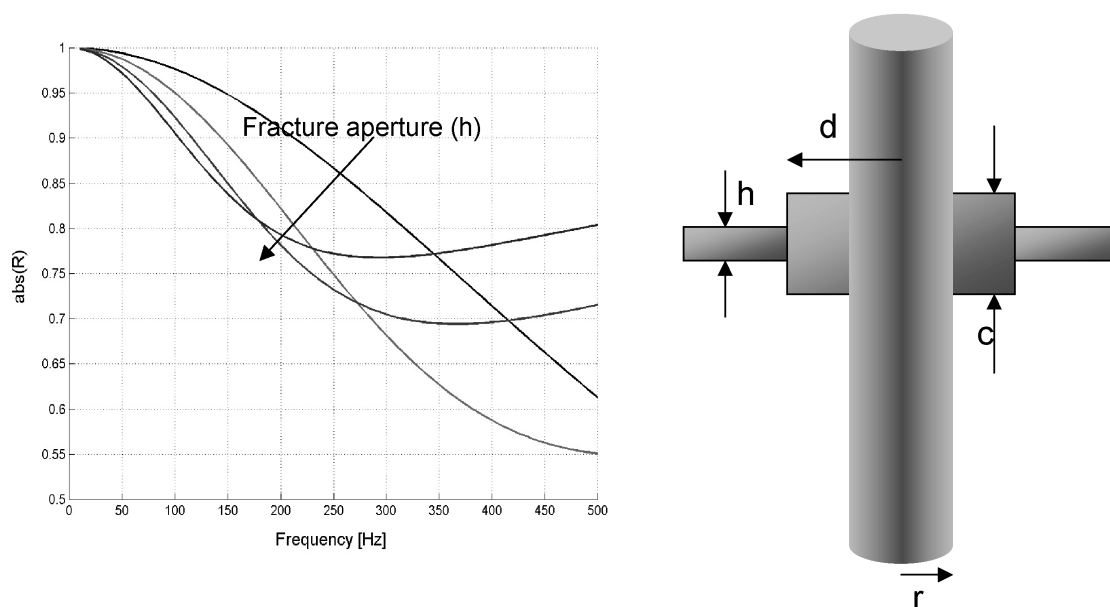
Fig. 10 - Spectral response of the amplitude of the reflection coefficient of the SW in a borehole with a wash out zone and discontinuity perpendicular to the borehole; the response was computed for different values of fracture aperture: Vst =1200 m/s (SW velocity); r=0.1 m (borehole radius); d=0.1 m (width of the washout zone); c=0.3 m (length of the washout along the borehole axis); h=0.01 - 0.05 - 0.1 - 0.15 m (fracture aperture).

5. Final remarks

The theoretical background of SW propagation in boreholes and its implication for geotechnical characterisation has been discussed, distinguishing between soft and hard rock. The analysis dealt with the relationship between the geometrical parameters of the borehole, the mechanical properties of the fluid that filled the borehole and the rock mass properties. The analysis, according to the approach proposed by the classical theory of a guided wave in a borehole (Biot, 1952), allows us to verify the sensitivity of the wave propagation for an uncased borehole in an isotropic rock mass. We developed a model to consider the radial anisotropy, i.e. due to the presence of plastic or metallic casing, the annulus material and the disturbance of the mechanical properties of the rock mass due to the drilling of the borehole. The model was adopted to study the discrepancy between the experimental data and the expected theoretical wave velocity in soft rock, where casing and annulus material are present, as in the first test site.

The second test, carried out in hard rock in a uncased borehole, permitted the reliability of the SW to detect fractures to be verified. In the data analysis, we considered that the diffusive effect was limited to high permeable fractures and negligible along the borehole in sound rock. Unfortunately, no reliable estimates of the shear modulus could be performed starting from the SW velocity, because of the evident effect of drilling disturbance in the second part of the borehole. The low velocity (around 800 m/s) is not compatible with the good quality of the rock mass, as indicated by the high values of the P-wave velocity (average around 3500 m/s). On the

other hand, the diffraction/reflection effects of the SW permitted the main fractures to be detected at least from a qualitative point of view. The conventional acquisition with hydrophones and pulse shots on the surface at low frequency (around 100 Hz) does not permit the application of more accurate quantitative interpretation because of the lack in sensitivity of the reflection coefficient to the aperture of the fracture.

Dispersion in soft rock does not seem useful in the low frequency range (below 1 kHz) in the conventional frequency band of downhole VSP acquisition to estimate the mechanical properties of rock; a wider acquisition band, up to 6 kHz, is required to use the dispersive behaviour of SWs.

The effect of casing and the annulus mechanical properties greatly affects the SW velocity. A more accurate interpretation of the SW propagation should consider the frame compressibility when a clay fraction is present in the rock matrix and the effect of fluid mobility in the porous medium.

REFERENCES

Alhilali K.A. and Zemanek J.; 1984: *Determination of formation permeability from a long-spaced acoustic log.* U.S. patent no. 4 432 077.

Biot M.A.; 1952: *Propagation of elastic waves in a cylindrical bore containing a fluid.* J. Appl. Phys., **23**, 997-1005.

Burns D.R., Tang X.M. and Reiter E.C.; 1992: *Estimating formation shear velocity from dispersive logging waveforms using a model-guided processing technique.* In: 62nd Ann. Internat. Mtg: Soc. of Expl. Geophys., pp. 205-208.

Cheng C.H. and Toksöz M.N.; 1981: *Elastic wave propagation in a fluid-filled borehole and synthetic acoustic logs.* Geophysics, **46**, 1042-1053.

Cheng C.H., Jinzhong Z. and Burns D.R.; 1987: *Effects of in-situ permeability on the propagation of Stoneley (tube) waves in a borehole.* Geophysics, **52**, 1279.

Godio A., Strobbia C. and De Bacco G.; 2006: *Geophysical characterisation of a rockslide in an alpine region.* Eng. Geol., **83**, 273-286

Hu L.Z. and McMechan G.A.; 1987: *Wave-field transformations of vertical seismic profiles.* Geophysics, **52**, 307-321.

Kostek S., Johnson D. L., Winkler K.W. and Hornby B.E.; 1998: *The interaction of tube waves with borehole fractures. Part II: Analytical models.* Geophysics, **63**, 809-815.

Mari J.L., Delay J., Gaudiani P. and Arens G.; 1996: *Geological formation characterization by SWs.* European Journ. of Env. and Eng. Geophys., **2**, 15-45.

Mathieu F.; 1984: *Application of full waveform acoustic logging data to the estimation of reservoir permeability.* M.Sc. thesis, MIT.

Norris A.N.; 1989: *Stoneley-wave attenuation and dispersion in permeable formations.* Geophysics, **54**, 330-341.

Paillet F.L. and White J.E.; 1982: *Acoustic modes of propagation in the borehole and their relationship to rock properties.* Geophysics, **47**, 1215-1228.

Renlie L. and Raaen A.M.; 1993: *Acoustic wave propagation in a fluid-filled borehole surrounded by a formation with stress-relief induced anisotropy.* Geophysics, **58**, 1257-1269.

Rosenbaum J.H.; 1974: S*ynthetic microseismograms - Logging in porous formations.* Geophysics, **39**, 14-32.

Schmitt D.P. and Bouchon M.; 1984: *Full wave synthetic acoustic logs in saturated porous media.* In: 54th Ann. Internat. Mtg: Soc. of Expl. Geophys., pp. 17-20.

Schmitt D.P., Bouchon M. and Bonnet G.; 1988: *Full-wave synthetic acoustic logs in radially semiinfinite saturated porous media.* Geophysics, **53**, 807-823.

Stevens J.L. and Day S.M.; 1986: *Shear velocity logging in slow formations using the SW.* Geophysics, **51**, 137-147.

Tang X.; 2002: *Determining formation shear-wave transverse isotropy from borehole Stoneley-wave measurements.* Geophysics, **68**, 118-126.

Tezuka K., Cheng C.H. and Tang X.M.; 1997: *Modeling of low-frequency Stoneley-wave propagation in an irregular borehole.* Geophysics, **62**, 1047-1058.

White J.E.; 1983: *Underground sound.* Elsevier Science Publ. Co., Amsterdam, 254 pp.

Winkler K.W.; 1985: *Dispersion analysis of velocity and attenuation in Berea sandstone.* J. Geophys. Res., **90**, 183.

Winkler K.W. and Murphy W.F.; 1995: *Acoustic velocity and attenuation in porous rock. Rock Physics and Phase Relations.* AGU, 20-34.

Appendix A

Low-frequency approximation for propagation of SWs along the *x*-axis of a fluid in a borehole in an isotropic (non permeable) medium could be derived according to Biot (1952):

$$\frac{\partial^2 V}{\partial x^2} - \frac{1}{a^2}\frac{\partial^2 V}{\partial t^2} = 0 \tag{A-1}$$

where the volume changing (V) along the borehole axis is related to the wave velocity of the fluid disturbance a:

$$a = \frac{\sqrt{K_f / \rho_f}}{\sqrt{1 + \frac{2K_f}{R}\frac{dR}{dp}}} \tag{A-2}$$

where K_f is the fluid compressibility modulus, ρf is the fluid density, R is the borehole radius and p is the pressure.

In an elastic formation, the changes in radius with respect to the pressure depends on the shear properties (G - shear modulus) of the medium:

$$\frac{dR}{dP} = \frac{R}{2G}$$

and therefore Eq. (A-2) yields:

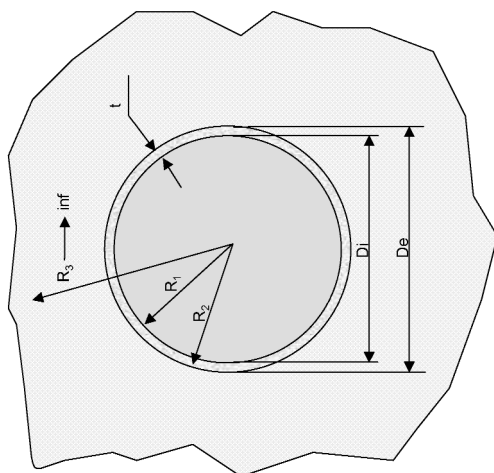$$a = \frac{\sqrt{K_f / \rho_f}}{\sqrt{1 + \frac{K_f}{G_m}}} \tag{A-3}$$

Fig. 11 - Sketch of the radial section of the borehole with casing and indication of different radii R1, R2 and R3 adopted in the relationship of Appendix A.

If we consider the presence of the thin casing and neglect the mechanical properties of the surrounding medium:

$$D \cdot dp = 2 \left(E \frac{dR}{R} \right) t$$

where E is the elasticity modulus and t is the thickness of the casing, it is possible to write

$$\frac{dR}{dp} = \frac{DR}{2Et}$$

and the tube wave velocity is the usual expression for water hammer in thin tubes:

$$a = \frac{\sqrt{K/\rho}}{\sqrt{1 + \dfrac{KD}{Et}}} \ .$$

For a casing under the hypothesis of a thin tube (Fig. 11), defining P_i as the inner pressure and P_e as the external pressure on the casing, which is equal to the pressure on the formation, we can write the expressions for the tube displacements and of the wall of the formation (Mariotte approach for the thin tube).

At a low frequency approximation, considering the axial variations negligible;
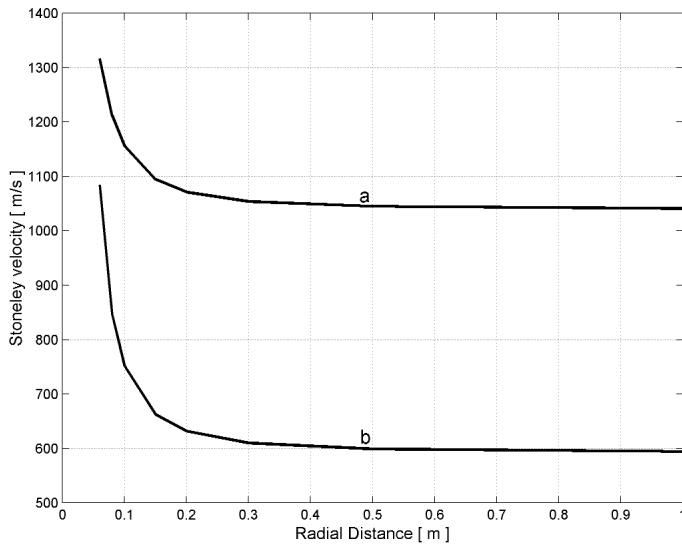
Fig. 12 - Computed response (see appendix A) of the SW velocity versus the radial distance form the borehole axis (borehole radius = 0.05 m) of the disturbed zone around the hole (E_2=40 GPa – Poisson coefficient = 0.25) in hard rock without casing: a) value of the Young modulus of the disturbed annulus – E_1=10 GPa, Poisson coefficient = 0.2; b) E_1=5 GPa, Poisson coefficient = 0.2;

$$\begin{cases} dR_e = \dfrac{R_e dP_e}{2G_f} \\ D_i dP_i - D_e dP_e = 2\left(E\dfrac{dR_i}{R_i} \right)t \end{cases}$$

the radial displacement of the formation and of the tube are:

$$dP_e = \frac{G_f dR}{R_e} \quad and \quad D_i dP_i - D_e \frac{G_f dR}{R_e} = 2E\frac{dR}{R_i}t$$

from which

$$dR = \left(\frac{D_i dP_i}{\dfrac{2Et}{R_i} + 4G} \right) \; .$$

We can write the expression for

$$\frac{dR}{dp} = \left(\frac{D_i}{\frac{2Et}{R_i} + 4G} \right) = \frac{D_i R_i}{2Et + 4GR_i}$$

and substituting in Eq. (A-2), the tube wave velocity is:

$$a = \frac{\sqrt{K/\rho}}{\sqrt{1 + \frac{2K}{R} \frac{DR}{2Et + 4GR}}} \quad a = \frac{\sqrt{K/\rho}}{\sqrt{1 + \frac{KD}{Et + 2GR}}} = \frac{V_f}{\sqrt{1 + \frac{KD}{Et + 2GR}}} \quad . \tag{A-5}$$

The term *dR/dp* in Eq. (A-2) can be derived for the case of a borehole with a casing where the thickness of the tube is not negligible with respect to the borehole radius; this simulates the presence of an annulus material around the borehole with different mechanical characteristics from the external medium (Fig. 12).

$$\frac{dR}{dp} = \frac{1}{2G_1 \left(R_2^2 - R_1^2 \right)} \left\{ \left[(1 - 2v1) R_1 R_2^2 + R_1 R_2^2 \right] \frac{dp_e}{dp} - \left[(1 - 2v_1) R_1^3 + R_1 R_2^2 \right] \right\} \tag{A-6}$$

if $R_3 \rightarrow \infty$

$$\frac{dp_e}{dp} = \frac{\left[\dfrac{R_1^2 R_2 (2 - 2v_1)}{2G_1 \left(R_2^2 - R_1^2 \right)} \right]}{\left[\dfrac{(1 - 2v_1) R_2^3}{2G_1 \left(R_2^2 - R_1^2 \right)} + \dfrac{R_1^2 R_2}{2G_1 \left(R_2^2 - R_1^2 \right)} + \dfrac{R_2}{G_2} \right]} \tag{A-7}$$

or

$$\frac{dp_e}{dp} = \frac{\dfrac{R_1^2 R_2 (2 - 2v_2)}{2G_1 \left(R_2^2 - R_1^2 \right)}}{\left[\dfrac{(1 - 2v_1) R_2^3}{2G_1 \left(R_2^2 - R_1^2 \right)} + \dfrac{R_1^2 R_2}{2G_1 \left(R_2^2 - R_1^2 \right)} + \dfrac{R_2 R_3^2}{2G_2 (R_3^2 - R_2^2)} + \dfrac{(1 - 2v_2) R_2^2}{2G_2 \left(R_3^2 - R_2^2 \right)} \right]} \quad . \tag{A-8}$$

Corresponding author: Alberto Godio
                          Politecnico di Torino
                          C.so Duca degli Abruzzi 24, 10129 Torino, Italy
                          e-mail: alberto.godio@polito.it